Relative latencies of cone signals measured by a moving vernier task

Zac Blake
Department of Experimental Psychology, Cambridge University, UK

Tom Land
Department of Experimental Psychology, Cambridge University, UK

John Mollon
Department of Experimental Psychology, Cambridge University, UK

When a bipartite blue and red bar is swept across a bright yellow field, the blue half of the bar appears to lag behind the red and to exhibit a longer persistence (J. D. Mollon & P. G. Polden, 1976). This effect has been taken to reveal the longer time constants of the short-wave channels of the visual system. In Experiment 1, we quantified the effect by a nulling technique: The average latency of the short-wave bar relative to the long-wave was 17.9 ms, and the average value for the relative persistence, i.e. the apparent temporal separation of the trailing edges of the bars, was 48.3 ms. However, the conditions of the original demonstration and those of Experiment 1 place the short-wave and long-wave channels in very different states: The yellow field produces little light adaptation in the short-wave cones, but polarizes opponent channels that carry short-wave signals. In Experiment 2 we selected an adapting field that equally raised the short- and long-wave mechanisms above their absolute thresholds but did not so strongly polarize post-receptoral channels. We adjusted the two stimuli to be equally above threshold on this field. When light adaptation and stimulus conditions were equated in these ways, there was very little difference either in the perceived latency or in the perceived duration of the short-wave and long-wave stimuli. We discuss possible reasons why different estimates of sensory latencies may be obtained from reaction times and from perceptual judgments.

Keywords: color vision, temporal vision, photoreceptors, latency, persistence of vision, motion in Maxwellian view

Citation: Blake, Z., Land, T., & Mollon, J. (2008). Relative latencies of cone signals measured by a moving vernier task. *Journal of Vision, 8*(16):16, 1–11, http://journalofvision.org/8/16/16/, doi:10.1167/8.16.16.

Introduction

As early as 1887, C. E. Stromeyer asked whether 'our perception of colour is slower for the blue and violet rays than for the green, yellow, and red ones'. During the twentieth century, Stromeyer's question took a modified form: Do the short-wave (S) cones respond more slowly than do the long- (L) and middle-wave (M) cones?

There is in fact rather little evidence that the short-wave cones themselves have longer time constants than the other cones. Schnapf, Nunn, Meister, and Baylor (1990) used suction electrodes to measure the membrane current of individual cone outer segments in macaque retina and reported that the kinetics and sensitivity of short-wave cones were similar to those of long- and middle-wave cones. And at the ganglion cell level, Yeh, Lee, and Kremers (1995) found similar temporal modulation transfer functions for +S–(L + M) and for +L–M and +M–L types of cell.

However, a relative delay of S-cone signals could arise later in the visual pathway. These signals are thought to be carried by small bistratified and large sparse monostratified ganglion cells (Dacey & Packer, 2003; Dacey, 2004), which project to the koniocellular laminae of the lateral geniculate nucleus, whereas signals from the L and M cones project to the magnocellular and parvocellular laminae. The koniocellular laminae are characterized by very small cell bodies, and Casagrande, Yazar, Jones, and Ding (2007) report that the koniocellular axons are of fine caliber compared to parvo- and magnocellular axons. Since conduction velocity is proportional to axon diameter, a delay to the S-cone signal could arise between the lateral geniculate and Area 17 of the cortex. It is interesting that Cottaris and De Valois (1998), recording from macaque cortical area V1, found S-opponent signals were available only after 96–135 ms, whereas L/M-opponent signals were available after 68–95 ms.

Several different psychophysical measures have suggested that the signals of the S cones are delayed relative to those of the long- and middle-wave cones. These measures include manual reaction times (e.g., McKeefry, Parry, & Murray, 2003; Mollon & Krauskopf, 1973), saccadic reaction times (e.g., Anderson, Husain, & Sumner, 2008; Bompas & Sumner, 2008; Perron & Hallett, 1995), chromatic discrimination of stimuli that modulate post-receptoral channels in different phase

doi: 10.1167/8.16.16 Received June 25, 2008; published December 29, 2008 ISSN 1534-7362

(Stromeyer, Eskew, Kronauer, & Spillmann, 1991), and two-pulse thresholds (Shinomori & Werner, 2006).

A phenomenon described by Mollon and Polden (1976) has often been used by lecturers and teachers to illustrate the delay of the short-wave cone signals. A slide projector is used to project on the screen an image of a thin vertical slit milled in a 50-mm square plate. One half of the slit is covered with a violet–blue filter (Wratten 47B) and the other with a long-pass filter (Wratten 25). The projector beam is reflected off a small mirror that is mounted on a galvanometer driven by a function generator. A Wratten 12 (or similar cut-on filter), mounted in a second slide projector, provides a bright yellow background field, which serves to ensure that the violet–blue component of the bipartite bar is visible only to the short-wave cones. When a sinusoidal or triangular waveform is supplied to the galvanometer, the bipartite bar is swept to and fro across the yellow background field.

Figure 1 depicts the striking appearance of the moving stimulus as reported by almost all observers: The blue component of the bar appears to lag the red component and also appears to persist longer. A good effect is obtained with a speed of 10 degrees of visual angle per second and with a slit that subtends 20 arcmin. Some effect may be seen with red and blue bars on a dark field (Charpentier, 1893; Ives, 1917; Stromeyer, 1887), but the differences in latency and persistence are more dramatic when the bright yellow field is introduced to isolate the short-wave cones.

Mollon and Polden's classroom demonstration has never been quantified, although it offers a direct way of measuring the relative delays of cone signals. In Experiment 1 we use a nulling technique (Ives, 1917) to quantify the effect. We measure relative latency by asking subjects to bring the leading edges of the red and blue bars into alignment; and we measure relative persistence by asking them to align the trailing edges. In Experiment 2 we ask whether the relative delay in the S-cone signal is still present when adaptive state and stimulus strength are equated for L and S cones.

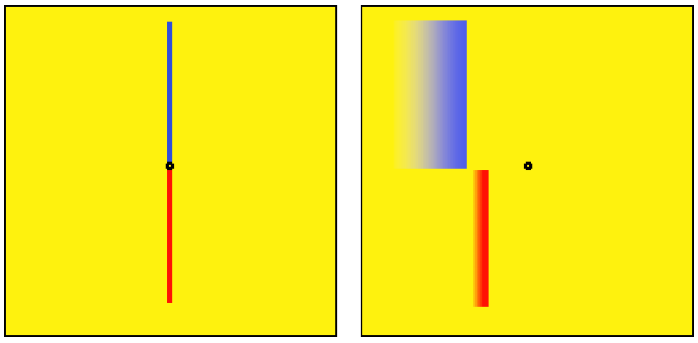

Figure 1. The Mollon–Polden effect. The left-hand panel shows the physical stimulus when the red and blue bars are stationary and aligned. The right-hand panel shows the appearance of this stimulus when in rightward motion. The subject fixates the center point.

Experiment 1: Methods

Subjects

There were 10 subjects, 5 male (age range 22–62) and 5 female (age range 21–30). All had normal color vision as measured by the Ishihara plates.

Apparatus

Stimuli were presented by means of a three-channel Maxwellian-view system with an exit pupil of 2 mm (Figure 2). Two beams provided the long-wave (600 nm; 6.91×10^9 quanta s^{-1} deg^{-2}) and short-wave (440 nm; 4.93×10^8 quanta s^{-1} deg^{-2}) components of the bipartite bar and a third provided a yellow background field (580 nm; 7.22×10^7 quanta s^{-1} deg^{-2}). Wavelengths were selected by blocked interference filters with full bandwidths at half height of 9.4–9.7 nm. The dimensions of each component bar were 4.3×0.19 degrees of visual angle. The background subtended 13×13 deg.

The bipartite bar stimulus was created by placing a machined aluminum device (Figure 3) with two opposed vertical slits in a collimated section of the common test beam. The lower slit was illuminated by short-wave light drawn from one beam and provided the upper bar as seen by the subject. The upper slit was illuminated by long-wave light from a second beam. The lower slit, cut into a slide mounted within a runner, could be moved laterally by means of a micrometer. The micrometer barrel was coupled to a stepping motor via a splined universal joint and thus could be controlled by a computer running MatLab.

To achieve movement of the bar across the field of view without motion of the Maxwellian image on the subject's pupil, we adopted an arrangement that was described by Burns and Webb (1994) and is illustrated in Figure 4. An image of the light source was formed on a small front-surface mirror, and this source image was relayed to the center of the subject's pupil. In the resting state, the mirror had an angle of 45° to the incident beam. When the slit device was introduced into the common test beam, a virtual image of the bars was produced by the collimating lens that followed the mirror. Small rotations of the mirror about a vertical axis (which passed through the source image) then resulted in lateral displacement of the virtual image of the bars without displacement of the source image in the plane of the subject's pupil. The rotation of the mirror was achieved by means of a galvanometer driven by a function generator with a triangular voltage output. The function generator also drove a shutter that hid the bars during half of the waveform, ensuring that motion was visible only from left to right in the observer's visual field. The rate of motion was 13 deg s^{-1} and the total extent was 13 deg.

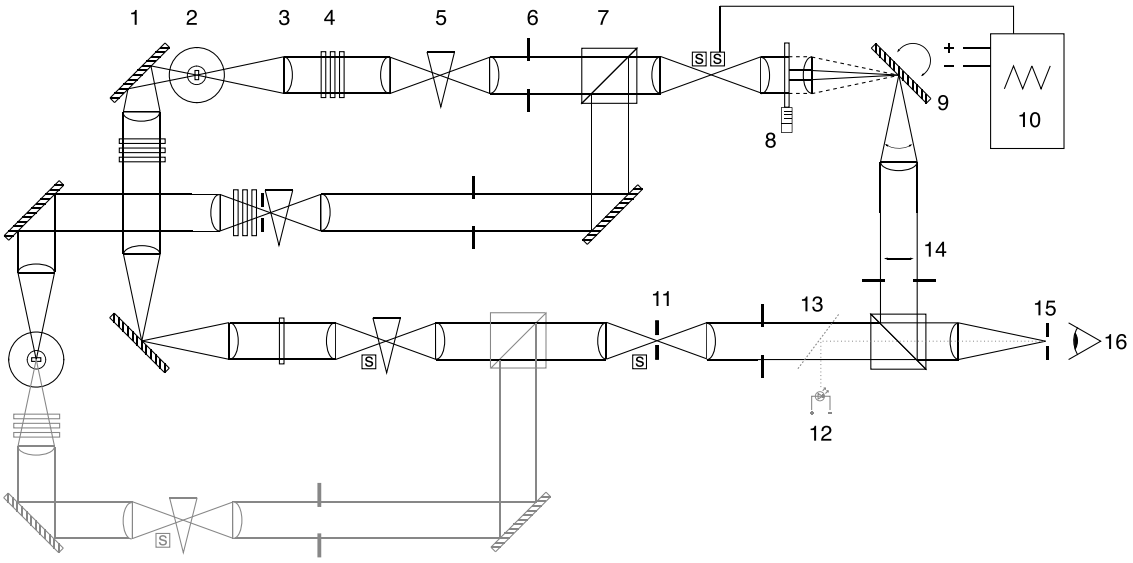

Figure 2. Schematic diagram of Maxwellian-view system used in both experiments. Shown in gray are additional components used in Experiment 2. Key: 1—Front-surface mirror; 2—Tungsten ribbon filament lamp; 3—Biconvex achromatic lens; 4—Fixed filters; 5—Circular neutral density wedge; 6—Field stop; 7—Beam-splitting cube; 8—Custom slit device; 9—Galvanometer-mounted front-surface mirror; 10—Function generator; 11—2-mm aperture; 12—Fixation LED [Experiment 2]; 13—Glass slide [Experiment 2]; 14—Position of test aperture for t.v.r. experiments [Experiment 2]; 15—Artificial pupil; 16—Observer.

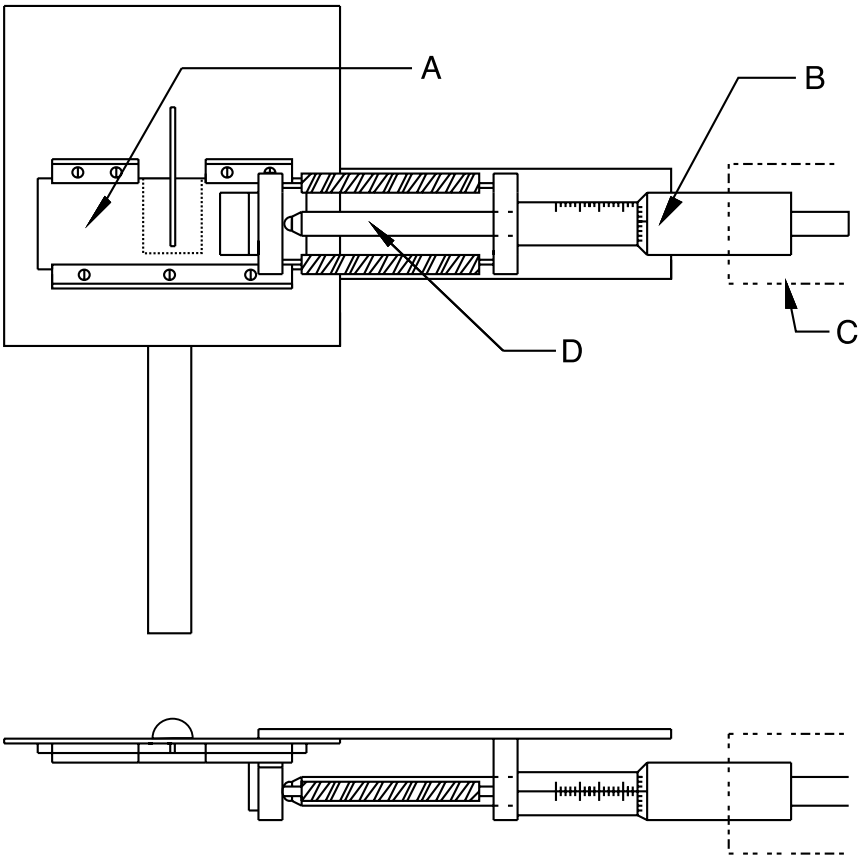

Figure 3. Orthographic projection showing the front elevation and plan views of the slit device used to produce the bipartite bar stimulus. A: Slide containing lower slit; B: Micrometer barrel; C: To stepping motor via a splined universal joint; D: Connecting rod incorporating sprung mechanism to eliminate backlash.

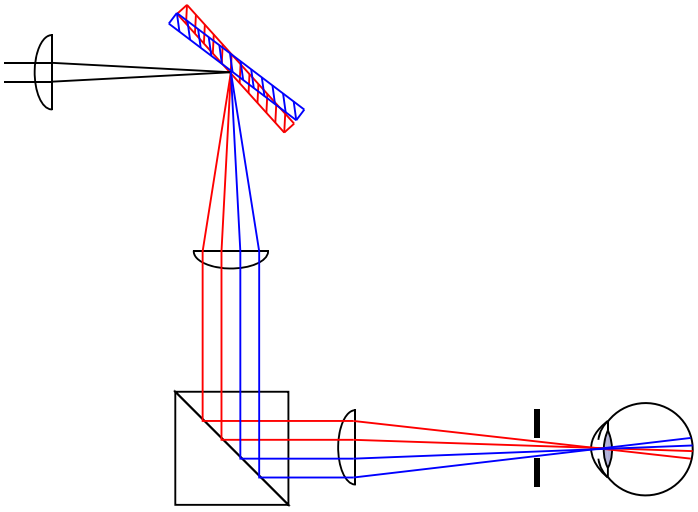

Figure 4. Technique for producing stimulus motion in Maxwellian view. The mirror position and the path of the light beam for two extremes of mirror rotation are illustrated in red and blue.

Calibrations were performed using a PIN10 silicon photodiode that had been calibrated by the National Physical Laboratory.

Procedure

The subject's eye position was stabilized by means of a mouth bite and was adjusted so that the subject's pupil was centered on the exit pupil of the apparatus. Ophthalmic lenses were placed just before the exit pupil to correct for individual refractive errors. Subjects used the eye that they preferred for looking through an aperture and their other eye was patched. They were asked to fixate a central fixation point at all times.

The relative latencies of the two bars were measured by a nulling technique similar to that used by Ives (1917). On any trial, the short-wave bar was physically offset from the long-wave bar by a certain distance and the subject was asked to indicate, by means of pushbuttons, which of the leading edges of the bars appeared to be in advance of the other. Subjects were asked to make their judgments as the stimulus passed the central fixation point. The physical offsets were adjusted according to a staircase routine programmed in MatLab. Two randomly interleaved staircases were used to prevent subjects anticipating the sequence of trials. The pair of interleaved staircases continued until they had each completed six reversals after crossing.

Before each set of measurements, subjects were asked to align the two bars while the bars were stationary in the center of the field, and this setting was taken to represent zero offset. After the end of each set of measurements, the program automatically returned the slits to this position, and the position was checked by the experimenter (no error was ever observed).

Two-minute adaptation to the background field preceded each set of measurements, and during this time the bipartite stimulus was hidden from view.

In separate runs, in order to measure the relative persistence of the two bars, subjects were asked to judge which of the trailing edges of the bars appeared to be in advance of the other.

The routine for each subject was as follows:

i. Two successive pairs of staircases were performed as training, one for the leading edges (L), one for the trailing edges (T).
ii. The subject had a 15-min break.
iii. Four successive pairs of staircases were performed in the sequence either LTLT or TLTL.
iv. The subject had a 15-min break.
v. Four successive pairs of staircases were performed in the opposite sequence to (iii).

Experiment 1: Results

In Figure 5, average settings are shown for each subject. The black symbols indicate the relative delay of the leading edge of the short-wave bar; and green symbols indicate the temporal separation between the trailing

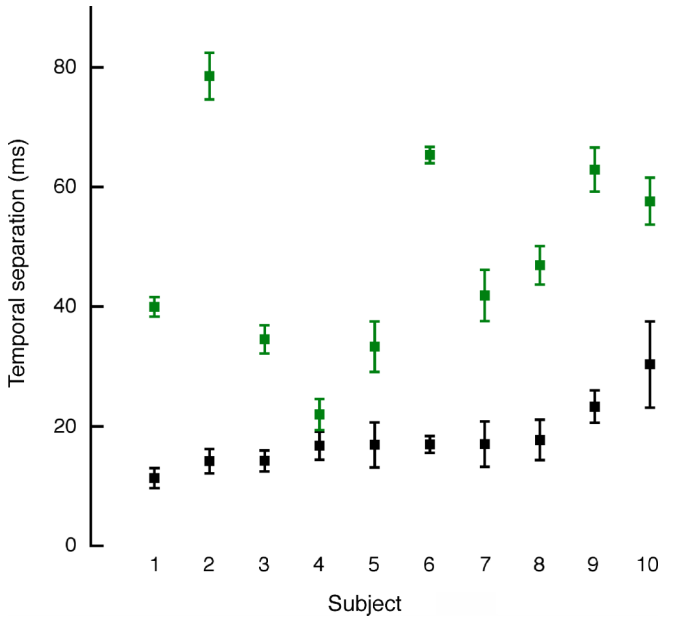

Figure 5. Results from Experiment 1. The black symbols show for each subject the average latency of the short-wave bar relative to that of the long-wave bar. The green symbols show the average temporal separation of the trailing edge of the short-wave bar relative to that of the long-wave bar. Error bars correspond to 1 *SEM*.

edges of the bars. Subjects are shown in order of increasing latency difference. Subjects 1, 3, 5, 6, and 9 are male.

The average latency of the short-wave bar relative to the long-wave was 17.9 ms. A *t*-test shows that this value is significantly different from zero ($t = 10.55$, $p < 0.0001$).

The average value for the temporal separation of the trailing edges of the bars was 48.3 ms. This value is significantly greater than the corresponding values for the latency of the leading edge ($t = 5.73$, $p < 0.001$), indicating that the short-wave stimulus has a longer apparent persistence under these conditions.

Subjects reported that judgments of the trailing edges were more difficult than were judgments of the leading edges, since the trailing edges were less well defined, especially in the case of the short-wave bar (as depicted in Figure 1).

Experiment 1: Discussion

Experiment 1 provides quantitative measurements of the phenomenon described qualitatively by Mollon and Polden (1976). All the subjects tested showed a measurably increased latency for the short-wave bar and all but one show a clearly longer visible persistence for the short-wave bar.

However, Experiment 1 does not necessarily show that the short-wave cones are systematically slower to respond than are the long-wave cones or that there are systematic delays in the pathways that carry the signals of the short-wave cones. Three factors must be taken into consideration:

i. In the original demonstration of Mollon and Polden and in Experiment 1, the short-wave and long-wave cones are not equally adapted by the yellow background field that is used to isolate the short-wave cone signal. And there is extensive evidence that the time constants of photoreceptors become shorter as light adaptation increases (Baylor & Hodgkin, 1974).

ii. Although the yellow background produces few photon absorptions in the short-wave cones themselves, it will strongly polarize the chromatically opponent channels that carry the short-wave signal. This 'second-site adaptation' (Polden & Mollon, 1980; Pugh & Mollon, 1979) may not only reduce the absolute sensitivity of the short-wave channels but may particularly reduce sensitivity to high temporal frequencies (Wisowaty & Boynton, 1980).

iii. The two test lights were of arbitrary radiance and originally chosen to provide a striking demonstration. But apparent latency is affected by stimulus radiance. Thus Guth (1964) presented a moving slit, fixed in radiance and wavelength, on a dark field, and asked his subjects to adjust the radiance of a second, physically collinear, moving slit until it appeared aligned with the first. His results suggested that slits of different color appeared aligned when they were set to the same luminance.

In Experiment 2 we aimed to compare the short-wave and long-wave signals under fairer conditions.

Experiment 2: Introduction

In this experiment we set out to select a background field that (i) placed the short- and long-wave cones in similar adaptive states, in so far as their thresholds were equally elevated above absolute threshold, and (ii) was as close to neutral as possible, in order to minimize any polarization of post-receptoral channels. In addition (iii), we wished to use stimulus radiances that were equally above the increment thresholds for the short- and long-wave cones. While satisfying the above requirements, we needed to ensure that the stimuli continued to isolate their target mechanisms.

In estimating the adapting field to be used in the latency measurements of Experiment 2, we first measured increment thresholds for parafoveal flashes according to the methods of Stiles (1949, 1978). In order to obtain thresholds appropriate for our moving bars as they passed the fixation point, we generated stimulus flashes by introducing a small fixed circular aperture into the path of either the red or the blue bar.

The adapting field (F_{crit}) that we used for our final measurements had two independently variable components: 550 nm (which had its primary effect on the long-wave cones) and 450 nm (which had its primary effect on the short-wave cones). These values were chosen on the basis of Stiles' field sensitivities (Wyszecki & Stiles, 1967) and of our own exploratory measurements.

To establish the absolute and incremental thresholds for each mechanism, we measured threshold vs. radiance (t.v.r.) curves on monochromatic and mixed backgrounds. Additionally, we measured the test spectral sensitivity for short-wave targets at both absolute and increment threshold, in order to confirm isolation of the short-wave cones.

For the final measurements of relative latency, we operationally equated the red and blue stimuli by raising each above its increment threshold by 0.2 log unit. However, if the two signals are carried by pathways with different contrast gains, an equal increment in intensity might not be translated into an equal increment in response. Any bias of this kind is likely to favor the long-wave cone signal, since the long-wave cones have access to channels, such as the magnocellular system, that have greater contrast gain (Kaplan & Shapley, 1986).

Experiment 2: Methods

Subjects

The subjects were the first two authors (subjects 9 and 6, respectively, from Experiment 1), who were experienced psychophysical subjects.

Apparatus

The apparatus used in Experiment 1 was modified to include a fourth beam, to be used either for rod adaptation before measurements of short-wave absolute thresholds or to provide a second component of the critical adapting field. In addition, shutters and circular neutral density wedges mounted on stepping motors were introduced into all beams, in order to allow measurements of t.v.r. curves.

To measure thresholds, a circular aperture of the same width as the test bar (0.2 deg) was introduced into the common test beam, either 1.5 deg above (short-wave flashes) or 1.5 deg below (long-wave flashes) the central fixation point. The parameters of stimulus movement were as for Experiment 1. A rectangular array of four points in the background field gave the subject additional guidance with respect to the positions of the flashes. When the background field was dim, the central fixation point was augmented by a dim red LED mounted behind a pinhole.

Procedure

The strategy for determining F_{crit} was as follows:

1. A t.v.r. curve was obtained for 650-nm flashes on a monochromatic 550-nm field, in order to obtain an estimate of the radiance of the 550-nm field required to raise the sensitivity of the long-wave cone mechanism by a criterion amount.
2. A partial t.v.r. curve for 440-nm flashes on a dim 550-nm field was obtained, in order to estimate the absolute threshold of the short-wave cones.
3. Spectral sensitivity measurements were made for test wavelengths between 420 nm and 480 nm in 10-nm increments on a dim 550-nm field. The purpose of these measurements was to ensure isolation of the short-wave cones near absolute threshold under the conditions of step 2.
4. A partial t.v.r curve was obtained for 440-nm flashes on a mixed background of a fixed 550-nm and varying 450-nm field. The 550-nm component was chosen such that the threshold for the 650-nm flash would be raised by 0.8 log units (from step 1 above).
5. Using the curves from steps 1 and 4 above, a composite field was constructed of 550-nm and 450-nm lights that raised the long- and short-wave test thresholds, respectively, by approximately 0.8 log units. The thresholds for both 440-nm and 650-nm flashes were then checked on this composite field, and further iterative corrections were made to the components to secure an approximately 0.8 log unit elevation for both test flashes (to a tolerance of ±0.05 log unit). This composite field, which elevates the thresholds for long- and short-wave targets by similar amounts, is the field that we refer to as F_{crit}.
6. Spectral sensitivity measurements were made for test wavelengths between 420 nm and 500 nm in 10-nm increments on the chosen composite field, to ensure that a suprathreshold short-wave test flash would still isolate the short-wave cones.

Each of steps 1–6 was repeated before moving on to the next step.

Measurements of t.v.r. curves were always made in order of ascending field radiance. Before a threshold measurement was made at each point on the t.v.r curves, the subject adapted for 2 min to the new adapting field. In steps 2 and 3 above, this was preceded by a 30-s presentation of a bright white field (7.1×10^5 td) intended to desensitize rods during the threshold measurements. During steps 3 and 6, short-wave test wavelengths were presented in a random order.

Every threshold was measured by a procedure in which two staircases were randomly interleaved. The stimulus was hidden from view between presentations and a warning tone preceded each presentation. The subject responded Seen or Not Seen. The pair of interleaved staircases continued until each had completed six reversals after crossing and the estimate of threshold was based on these reversals.

In order to make the measurements of latency, the aperture was removed from the common test beam, and the short- and long-wave bars were set to be 0.2 log units above their respective thresholds on the composite field.

The procedure for latency measurements was as for Experiment 1. Six independent measurements were made for leading edges and 6 for trailing edges, in alternating sequence.

Experiment 2: Results

Choice of F_{crit}

In Figure 6 we present for each subject the results that were used to select F_{crit}. Graph A (open red circles) represents the t.v.r. curve for 650-nm flashes on a 550-nm background of increasing radiance. Since the long-wave cones have a test sensitivity greater than the middle-wave cones by 0.65 log unit at 650 nm and since the field

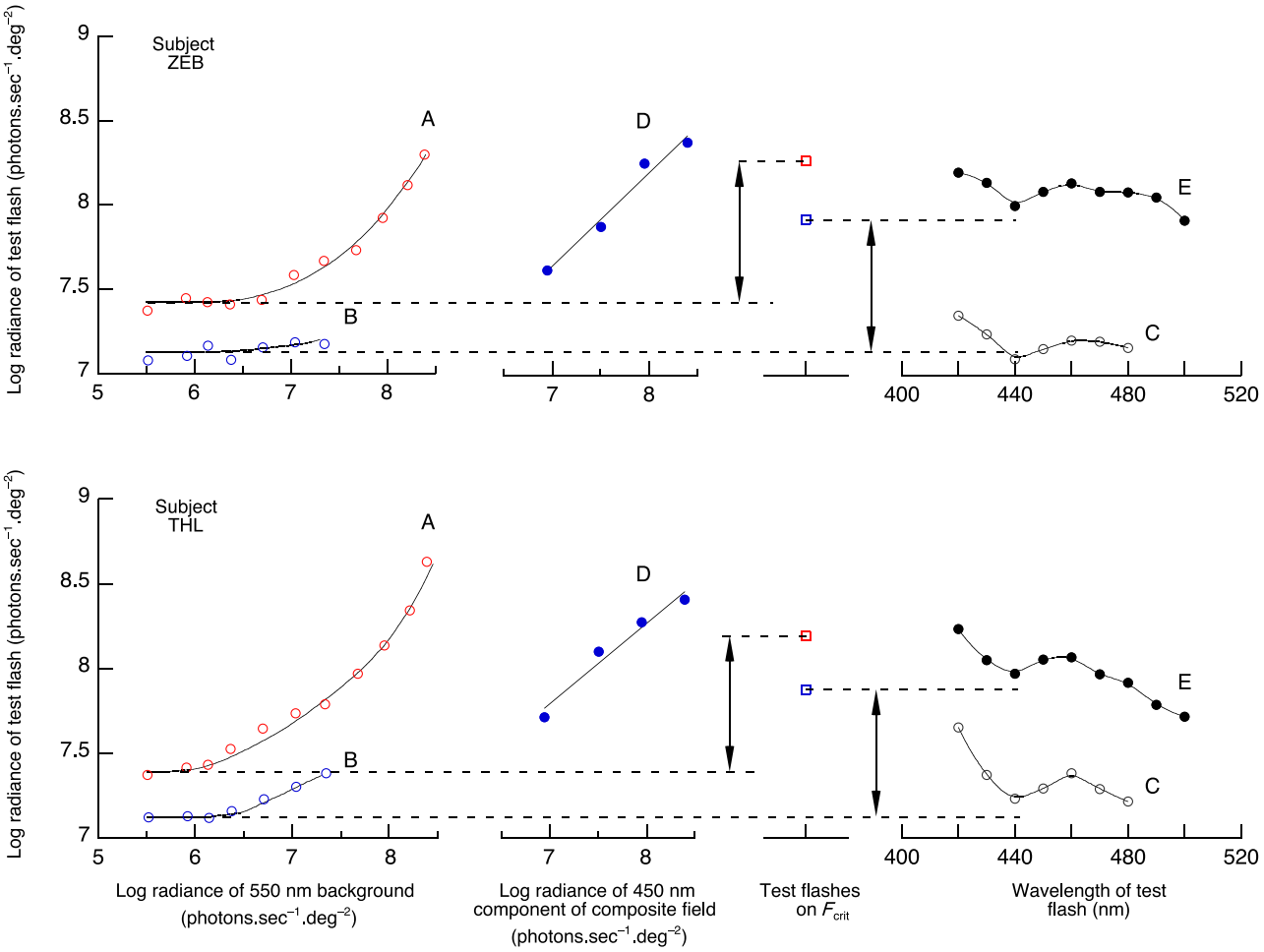

Figure 6. Results of experiments used to select F_{crit} for subjects ZEB and THL. See text for full explanation. *Graph A* (red open circles): thresholds for 650-nm flashes on a 550-nm background of increasing radiance. *Graph B* (blue open circles): thresholds for 440-nm flashes on a 550-nm background of increasing radiance. *Graph C* (open black circles): reciprocal spectral sensitivities (thresholds vs. wavelength) on a dim 550-nm field. A horizontal dashed line connects the measured value at λ = 440 nm with the independently obtained value for the same conditions in the t.v.r. curve of Graph B. *Graph D* (filled blue circles): partial t.v.r curve for 440-nm flashes on a composite background comprising a variable 450-nm component and a fixed 550-nm component. The radiance of the 550-nm component was that required to raise the detection threshold in Graph A by 0.8 log units. To the right of Graph D are shown (red and blue open squares) the thresholds for the long-wave and short-wave targets on the composite field, F_{crit}, used for the final latency measurements. *Graph E* (solid black circles): thresholds vs. wavelength for short-wave flashes presented on F_{crit}.

sensitivity at 550 nm is similar for the two classes of cone (Wyszecki & Stiles, 1967), the test flashes will be detected by long-wave cones throughout the curve.

Graph B (open blue circles) represents the thresholds for 440-nm test flashes on dim 550-nm fields: These are the data used to estimate the absolute threshold for the short-wave cones. Graph C (open black circles) shows thresholds as a function of test wavelength in the short-wave region: A minimum of threshold in the region of 440 nm confirms isolation of the short-wave cones.

Graph D (closed blue circles) shows a partial t.v.r. graph for 440-nm test flashes on a composite background comprising a variable 450-nm component and a fixed 550-nm component derived from the point on Graph A at which the 650-nm test threshold was elevated by 0.8 log unit. From this curve we took an initial candidate for the required composite field. However, we consistently found that this composite field raised the 650-nm threshold less than did the 550-nm component alone. We therefore made small iterative adjustments to both components until approximately 0.8 log unit threshold elevations were achieved for both the 650-nm and the 440-nm test flashes. The final composite fields for ZEB were 3.72×10^7 450-nm photons s^{-1} deg^{-2} and 2.47×10^8 550-nm photons s^{-1} deg^{-2} raising the long- and short-wave test detection thresholds by 0.839 and 0.784 log unit, respectively. F_{crit} for THL was found to be 1.89×10^7 450-nm photons s^{-1} deg^{-2} and 1.16×10^8 550-nm photons s^{-1} deg^{-2}, raising the long- and short-wave test detection thresholds

by 0.803 and 0.754 log unit, respectively. The CIE (1931) chromaticities of these fields were $x = 0.270$, $y = 0.547$ for ZEB and $x = 0.268$, $y = 0.537$ for THL. The corresponding MacLeod and Boynton (1979) chromaticity coordinates were 0.6097, 0.0045 and 0.6096, 0.0048. Subjectively, the fields appeared in a desaturated pistachio color.

Graph E (solid black circles) shows thresholds as a function of test wavelength on the final composite field: A minimum of threshold in the region of 440 nm confirms isolation of the short-wave cones.

Relative latency and persistence measured on F_{crit}

To make our final latency measurements using the bar stimuli, we set the 440- and 650-nm test radiances to be 0.2 log units above their increment thresholds on the composite field. By reference to Stiles' π_4 sensitivity (Wyszecki & Stiles, 1967, Tables 7.4 and 7.6) and the spectral sensitivity at threshold shown for each observer in Graph E, we can be confident that the short-wave cone signal remained isolated at this test radiance.

Table 1 shows in milliseconds the relative latencies for leading and trailing edges when the moving bars were presented on the composite field. For ZEB the leading edge discrepancy does not significantly differ from zero ($t = 0.833$, $p = 0.44$) and for THL there is only a very small and marginally significant delay for the short-wave stimulus ($t = 3.359$, $p = 0.02$).

For both subjects, the absolute value of the offset of the short-wave *trailing* edge is significantly different from zero (Table 1; $t = 6.2$, $p = 0.0016$, in both cases). If we estimate persistence by comparing the trailing-edge measurements with the leading-edge measurements (as for Experiment 1 above), then ZEB shows a significantly increased persistence for the short-wave cones ($t = 3.48$, $p = 0.006$), but THL does not ($t = 0.71$, $p = 0.5$). The conclusion we wish to emphasize is that the residual difference between trailing edges is very small: The short- and long-wave stimuli have similar persistences when the critical adapting field is present.

	Leading edge		Trailing edge	
Subject	Relative delay (ms)	*SD*	Relative delay (ms)	*SD*
ZEB	0.73	2.15	4.81	1.90
THL	2.74	2.00	3.44	1.37

Table 1. Mean values for the relative delays (in milliseconds) of the leading and trailing edges of the bipartite bar when moving across a field that similarly adapts the long-wave and short-wave cones (Experiment 2). Each mean is based on six independent measurements. Positive values indicate that the short-wave component of the bar is lagging.

Experiment 2: Discussion

When the playing field is level, i.e. when the adaptive states of the cones are similar, when post-receptoral sites are not strongly polarized, and when the stimuli are equally above threshold, the signals from the long- and short-wave cones are perceived as having very similar latencies. Therefore, the original Mollon–Polden effect should not be used to persuade students and other audiences that the short-wave cones have longer time constants. The effect does still have an honest place in the classroom: It demonstrates rather vividly that physically simultaneous events do not necessarily appear simultaneous in our perceptual awareness, and it remains one of the easier ways of making this point to a student audience.

F_{crit} is the field that we found to elevate thresholds similarly for short-wave and long-wave cone stimuli. Its chromaticity would lie on the margin of the gamut of real-world surfaces observed under Illuminant D65 (Nascimento, Ferreira, & Foster, 2002) and does not correspond to the chromaticity of, say, an equal-energy white. We emphasize that it is simply the field found empirically to reduce sensitivity by similar amounts for stimuli that isolate the short-wave and long-wave cones.

The alternative measures of sensory latency

Our conclusions are restricted to the particular response measure that we used. Bompas and Sumner (2008) have shown that perceptual judgments of temporal order show little difference between short-wave and achromatic stimuli, under experimental conditions where a substantial short-wave delay is seen for manual and saccadic responses. Their finding reflects earlier observations that judgments of temporal order are rather little affected by changes in stimulus parameters (such as luminance, spatial frequency) that bring large changes in reaction time (Cardoso-Leite, Gorea, & Mamassian, 2007; Tappe, Niepel, & Neumann, 1994).

There are at least three reasons why different estimates of relative latency will be obtained with different response measures:

The plurality of pathways

There are known to be at least fifteen morphologically and functionally distinct types of retinal ganglion cell, each with their own specific central projections (Dacey, 2004; Dacey, Peterson, Robinson, & Gamlin, 2003; Petrusca et al., 2007). The different types draw different combinations of inputs from the cones and with different weightings and different contrast gains. So it is very likely that the apparent relative latencies of long-wave and short-wave cone signals will be different according to the

response measure that is used and according to the intensities of the stimuli relative to threshold. In particular, signals from the short-wave cones may chiefly be carried by chromatically opponent channels and may have little or no access to the transiently responding parasol and upsilon types of ganglion cell or to mid-brain projections (de Monasterio, 1978a, 1978b; Gouras, 1968; Petrusca et al., 2007; Schiller & Malpeli, 1977). This has traditionally been taken to be one factor leading to longer reaction times for liminal short-wave increments compared to long-wave increments (Mollon, 1982; Mollon & Krauskopf, 1973). Using an adapting field metameric to equal-energy white and using luminance noise to isolate chromatic channels, Smithson and Mollon (2004) found that two subjects showed no difference in reaction times to liminal S/(L + M) and L/(L + M) signals while a third subject showed a mean difference of 13 ms.

Different measures tap different aspects of the neural response

A manual or saccadic reaction to a suprathreshold stimulus can in principle be triggered as soon as the neural response to the signal exceeds the background response by a criterion amount and so will depend on the earliest components of the neural response (Lennie, 1981), but a phenomenological judgment of the time at which a stimulus occurs is unlikely to be based on the earliest components alone.

Calibration of phenomenological judgments

Our task, like temporal order judgments, requires the observer to make a conscious perceptual assessment. Human beings have evolved to make reactions that are as swift as possible but to make perceptual judgments that are as accurate as possible. It would be as unsatisfactory for our order judgments to be affected by peripheral transmission times as it would be for our spatial vernier judgments to be affected by distortions of the retinal image. It is true that subjects experience illusions, in space and in time, especially when they are tested under stimulus conditions that they seldom experience in the real world. But it is an almost universal law that the illusions will dissolve if the subjects are given extended practice and are allowed to calibrate themselves, ideally by interacting with the stimuli (Lewis, 1908).

Many a visual scientist would adopt a position of this kind with respect to *spatial* distortion. For there are plenty of demonstrations that imposed spatial distortions become invisible with practice and that perceptual judgments regain their accuracy (Welch, 1979). Yet the same visual scientist may be unwilling to accept that such is also the case for *temporal* perception. Behind this reluctance may be an implicit model in which sensory events are delivered, centrally and are experienced in the theater of consciousness, in the order that they arrive. In fact, our short-term visual experience is better thought of as trafalmadorian: The iconic store, which we examine when asked to make a perceptual judgment, is probably four-dimensional, in that time is represented within it (Smithson & Mollon, 2006). If this is the case, then it is reasonable to expect that our perception of temporal sequence is calibrated by interaction with the world.

In our everyday experience, moving white or purple objects do not break up into their component colors. Nor do their high spatial frequency components trail behind their low spatial frequency structure. Nor are their colors dissociated from their other attributes. Our temporal perceptions are designed to be veridical even if transmission times are different for different pathways. In extreme stimulus conditions, such as those of the original Mollon–Polden effect, illusions may occur, but in most circumstances the process of perceptual synthesis—the recombination of attributes of a particular object—occurs as reliably in time as it does in space.

Acknowledgments

Commercial relationships: none.
Corresponding author: John D. Mollon.
Email: jm123@cam.ac.uk.
Address: Department of Experimental Psychology, University of Cambridge, Downing St., Cambridge CB2 3EB, United Kingdom.

References

Anderson, E. J., Husain, M., & Sumner, P. (2008). Human intraparietal sulcus (IPS) and competition between exogenous and endogenous saccade plans. *Neuroimage, 40,* 838–851. [PubMed]

Baylor, D. A., & Hodgkin, A. L. (1974). Changes in time scale and sensitivity in turtle photoreceptors. *The Journal of Physiology, 242,* 729–758. [PubMed] [Article]

Bompas, A., & Sumner, P. (2008). Sensory sluggishness dissociates saccadic, manual, and perceptual responses: An S-cone study. *Journal of Vision, 8*(8):10, 1–13, http://journalofvision.org/8/8/10/, doi:10.1167/8.8.10. [PubMed] [Article]

Burns, S. A., & Webb, R. H. (1994). Optical generation of the visual stimulus. In M. Bass, E. W. van Stryland, D. R. Williams, & W. I. Wolfe (Eds.), *The handbook of optics* (pp. 1–27). New York: McGraw Hill.

Cardoso-Leite, P., Gorea, A., & Mamassian, P. (2007). Temporal order judgment and simple reaction times: Evidence for a common processing system. *Journal of Vision, 7*(6):11, 1–14, http://journalofvision.org/7/6/11/, doi:10.1167/7.6.11. [PubMed] [Article]

Casagrande, V. A., Yazar, F., Jones, K. D., & Ding, Y. (2007). The morphology of the koniocellular axon pathway in the macaque monkey. *Cerebral Cortex, 17,* 2334–2345. [PubMed] [Article]

Charpentier, A. (1893). Démonstration directe de la différence de temps perdu suivant les couleurs. *Archives de Physiologie, 5,* 568–570.

Cottaris, N. P., & De Valois, R. L. (1998). Temporal dynamics of chromatic tuning in macaque primary visual cortex. *Nature, 395,* 896–900. [PubMed]

Dacey, D. M., & Packer, O. S. (2003). Colour coding in the primate retina: Diverse cell types and cone-specific circuitry. *Current Opinion in Neurobiology, 13,* 421–427. [PubMed]

Dacey, D. M. (2004). Origins of perception: Retinal ganglion cell diversity and the creation of parallel visual pathways. In M. S. Gazzaniga (Ed.), *The cognitive neurosciences* (pp. 281–301). Cambridge, MA: MIT.

Dacey, D. M., Peterson, B. B., Robinson, F. R., & Gamlin, P. D. (2003). Fireworks in the primate retina: In vitro photodynamics reveals diverse LGN-projecting ganglion cell types. *Neuron, 37,* 15–27. [PubMed] [Article]

de Monasterio, F. M. (1978a). Center and surround mechanisms of opponent-color X and Y ganglion cells of retina of macaques. *Journal of Neurophysiology, 41,* 1418–1434. [PubMed]

de Monasterio, F. M. (1978b). Properties of concentrically organised X and Y ganglion cells of macaque retina. *Journal of Neurophysiology, 41,* 1394–1417. [PubMed]

Gouras, P. (1968). Identification of cone mechanisms in monkey ganglion cells. *The Journal of Physiology, 199,* 535–547. [PubMed] [Article]

Guth, S. L. (1964). The effect of wavelength on visual perceptual latency. *Vision Research, 4,* 567–578. [PubMed]

Ives, H. E. (1917). Visual diffusivity. *Philosophical Magazine, 33,* 18–33.

Kaplan, E., & Shapley, R. M. (1986). The primate retina contains two types of ganglion cells, with high and low contrast sensitivity. *Proceedings of the National Academy of Sciences of the United States of America, 83,* 2755–2757. [PubMed] [Article]

Lennie, P. (1981). The physiological basis of variations in visual latency. *Vision Research, 21,* 815–824. [PubMed]

Lewis, E. O. (1908). The effect of practice on the perception of the Müller–Lyer illusion. *British Journal of Psychology, 2,* 294–306.

MacLeod, D. I., & Boynton, R. M. (1979). Chromaticity diagram showing cone excitation by stimuli of equal luminance. *Journal of the Optical Society of America, 69,* 1183–1186. [PubMed]

McKeefry, D. J., Parry, N. R., & Murray, I. J. (2003). Simple reaction times in color space: The influence of chromaticity, contrast, and cone opponency. *Investigative Ophthalmology & Visual Science, 44,* 2267–2276. [PubMed] [Article]

Mollon, J. D. (1982). A taxonomy of tritanopias. In G. Verriest (Ed.), *Colour vision deficiencies* (vol. VI, pp. 87–101). The Hague: Dr. W. Junk.

Mollon, J. D., & Krauskopf, J. (1973). Reaction time as a measure of the temporal response properties of individual colour mechanisms. *Vision Research, 13,* 27–40. [PubMed]

Mollon, J. D., & Polden, P. G. (1976). Proceedings: Some properties of the blue cone mechanism of the eye. *The Journal of Physiology, 254,* 1P–2P. [PubMed] [Article]

Nascimento, S. M., Ferreira, F. P., & Foster, D. H. (2002). Statistics of spatial cone-excitation ratios in natural scenes. *Journal of the Optical Society of America A, Optics, Image Science, and Vision, 19,* 1484–1490. [PubMed] [Article]

Perron, C., & Hallett, P. E. (1995). Saccades to large coloured targets stepping in open fields. *Vision Research, 35,* 263–274. [PubMed]

Petrusca, D., Grivich, M. I., Sher, A., Field, G. D., Gauthier, J. L., Greschner, M., et al. (2007). Identification and characterization of a Y-like primate retinal ganglion cell type. *Journal of Neuroscience, 27,* 11019–11027. [PubMed] [Article]

Polden, P. G., & Mollon, J. D. (1980). Reversed effect of adapting stimuli on visual sensitivity. *Proceedings of the Royal Society of London B: Biological Sciences, 210,* 235–272. [PubMed]

Pugh, E. N., Jr., & Mollon, J. D. (1979). A theory of the pi1 and pi3 color mechanisms of Stiles. *Vision Research, 19,* 293–312. [PubMed]

Schiller, P. H., & Malpeli, J. G. (1977). Properties and tectal projections of monkey retinal ganglion cells. *Journal of Neurophysiology, 40,* 428–445. [PubMed]

Schnapf, J. L., Nunn, B. J., Meister, M., & Baylor, D. A. (1990). Visual transduction in cones of the monkey *Macaca fascicularis*. *The Journal of Physiology, 427,* 681–713. [PubMed] [Article]

Shinomori, K., & Werner, J. S. (2006). Impulse response of an S-cone pathway in the aging visual system. *Journal of the Optical Society of America A, Optics, Image Science, and Vision, 23,* 1570–1577. [PubMed] [Article]

Smithson, H., & Mollon, J. (2006). Do masks terminate the icon? *Quarterly Journal of Experimental Psychology, 59,* 150–160. [PubMed]

Smithson, H. E., & Mollon, J. D. (2004). Is the S-opponent chromatic sub-system sluggish? *Vision Research, 44,* 2919–2929. [PubMed]

Stiles, W. S. (1949). Increment thresholds and the mechanisms of colour vision. *Documenta Ophthalmologica, 3,* 138–165. [PubMed]

Stiles, W. S. (1978). *Mechanisms of colour vision*. London: Academic Press.

Stromeyer, C. E. (1887). The perception of colour. *Nature, 35,* 246.

Stromeyer, C. F., III, Eskew, R. T., Jr., Kronauer, R. E., & Spillmann, L. (1991). Temporal phase response of the short-wave cone signal for color and luminance. *Vision Research, 31,* 787–803. [PubMed]

Tappe, T., Niepel, M., & Neumann, O. (1994). A dissociation between reaction time to sinusoidal gratings and temporal-order judgment. *Perception, 23,* 335–347. [PubMed]

Welch, R. B. (1979). *Perceptual modification*. New York: Academic Press.

Wisowaty, J. J., & Boynton, R. M. (1980). Temporal modulation sensitivity of the blue mechanism: Measurements made without chromatic adaptation. *Vision Research, 20,* 895–909. [PubMed]

Wyszecki, G., & Stiles, W. S. (1967). *Color science*. New York: Wiley.

Yeh, T., Lee, B. B., & Kremers, J. (1995). Temporal responses of ganglion cells of the macaque retina to cone-specific modulation. *Journal of the Optical Society of America A, 12,* 456–464.